

## Article

# Dual-Pump Vibrational Coherent Anti-Stokes Raman Scattering System Developed for Simultaneous Temperature and Relative Nitrogen–Water Vapor Concentration Measurements

Amon Too <sup>1,2,3,4</sup>, Evaggelos Sidiropoulos <sup>1,2</sup>, Yannik Holz <sup>1,2</sup>, Nancy Wangechi Karuri <sup>3</sup> and Thomas Seeger <sup>1,2,\*</sup> 

<sup>1</sup> Institute of Engineering Thermodynamics, University of Siegen, 57076 Siegen, Germany; too.amon21@students.dkut.ac.ke (A.T.); evaggelos.sidiropoulos@uni-siegen.de (E.S.); yannik.holz@googlemail.com (Y.H.)

<sup>2</sup> Center for Sensor Systems (ZESS), University of Siegen, 57076 Siegen, Germany

<sup>3</sup> Department of Chemical Engineering, Dedan Kimathi University of Technology, Nyeri 10143, Kenya; nancy.karuri@dkut.ac.ke

<sup>4</sup> Department of Mechanical Engineering, Dedan Kimathi University of Technology, Nyeri 10143, Kenya

\* Correspondence: thomas.seeger@uni-siegen.de; Tel.: +49-271-740-3124

**Abstract:** Simultaneous gas phase temperature and water vapor concentration measurement are important to understand reacting flows such as combustion or gas reforming processes. Here, coherent anti-Stokes Raman scattering (CARS) offers the possibility for non-intrusive measurements with a high temporal and spatial resolution. Therefore, this work demonstrates the simultaneous measurement of temperature and relative water vapor–nitrogen concentrations by using dual-pump vibrational coherent anti-Stokes Raman scattering (DPVCARS). A calibration procedure is developed for a temperature range of 473 K to 673 K and a water vapor concentration of 24% to 46% at ambient pressure. This setup is tested with 500 CARS single pulse spectra taken in a gas cell at a known temperature and concentration. Based on these results, information about precision and accuracy can be delivered.



**Citation:** Too, A.; Sidiropoulos, E.; Holz, Y.; Karuri, N.W.; Seeger, T. Dual-Pump Vibrational Coherent Anti-Stokes Raman Scattering System Developed for Simultaneous Temperature and Relative Nitrogen–Water Vapor Concentration Measurements. *Optics* **2023**, *4*, 613–624. <https://doi.org/10.3390/opt4040046>

Academic Editor: Yuriy Garbovskiy

Received: 14 October 2023

Revised: 19 November 2023

Accepted: 4 December 2023

Published: 8 December 2023



**Copyright:** © 2023 by the authors. Licensee MDPI, Basel, Switzerland. This article is an open access article distributed under the terms and conditions of the Creative Commons Attribution (CC BY) license (<https://creativecommons.org/licenses/by/4.0/>).

**Keywords:** vibrational coherent anti-stokes Raman scattering (VCARS); dual-pump VCARS; laser diagnostic; temperature measurement; concentration measurement

## 1. Introduction

For a fundamental understanding of reactive flows, simultaneous temperature and species concentration information is of utmost importance. Here, water vapor is the major product of hydrogen combustion and often the dominant product species of hydrocarbon-fueled combustion processes. Water vapor is also an important molecule in reforming processes, in particular synthetic methanation. Here hydrogen, e.g., produced from excess renewable energy, is reacted with carbon dioxide in the presence of a catalyst and chemically transformed to methane, which can be stored and transported through the well-developed natural gas infrastructure already in place [1,2]. In this process, water vapor is one of the main products, and, therefore, its concentration can be essential in determining the degree of conversion achieved [3,4]. However, to understand and optimize a dynamic process like synthetic methanation, it requires accurate operando temperature and relative concentration measurements. Conventional gas sampling probes are intrusive with low spatial and temporal resolution, and as such, they are unreliable for use in a dynamic reaction [5]. Therefore, fast, laser-based optical diagnostic techniques are more suitable. For this task, Raman spectroscopic techniques are ideally suited because of the species-selective character and the number density dependence of the Raman scattering process [1,5,6]. For time-resolved temperature and water vapor measurements with the spontaneous Raman scattering technique at elevated temperatures and ambient pressure, high laser intensities and large-aperture windows for the signal collection path are necessary, which limit the use

of this technique [7,8]. Today, the coherent anti-Stokes Raman (CARS) technique is routinely used for temperature determination, even in harsh combustion environments such as an IC engine, coal furnace, high-pressure burner, and rotating detonation combustor [9–12]. The precision of temperature measurements using N<sub>2</sub> vibrational CARS (VCARS) has already been well investigated in several studies, providing a measurement inaccuracy of 2–5% at elevated temperatures (see, e.g., [13]).

The dual-pump vibrational CARS (DPVCARS) technique has especially been developed for simultaneous temperature and multispecies concentration measurements in reacting flows. This technique has been used for simultaneous temperature and N<sub>2</sub>-O<sub>2</sub> concentration measurements [14–16], as well as N<sub>2</sub>-CO<sub>2</sub> concentration measurements [17,18]. Also, hydrocarbon-based fuel molecules and N<sub>2</sub> have been detected simultaneously (N<sub>2</sub>-C<sub>3</sub>H<sub>8</sub> [14], N<sub>2</sub>-CH<sub>3</sub>OH [17], and N<sub>2</sub>-CH<sub>4</sub> [19]). In addition, simultaneous temperature and concentration measurements for up to three species in flames have been demonstrated with this technique (e.g., N<sub>2</sub>, O<sub>2</sub>, C<sub>2</sub>H<sub>4</sub> [20], N<sub>2</sub>, O<sub>2</sub>, CO [21], or N<sub>2</sub>, CO, H<sub>2</sub> [22]). The detection of even more molecules has already been shown [23]. A major advantage of the DPVCARS technique is that the CARS signal of each molecule is generated by all three laser beams. As a result, energy intensity fluctuations in the laser beams are not relevant since relative species concentrations are measured. Nevertheless, up until now, DPVCARS has not been used for simultaneous temperature and water vapor concentration measurements.

The first measurements of a VCARS spectrum of water vapor have been performed by Hall et al. [24]. The experimental H<sub>2</sub>O spectrum achieved in a premixed methane-air flame was compared to a calculated spectrum at 1675 K. The calculation is based on several approximations. It is restricted to isotropic Q-branch transitions; the non-resonant susceptibility was assumed to be equal to that of N<sub>2</sub>, and for all transitions, homogeneous Raman linewidths of 0.1 cm<sup>-1</sup> were used. Especially the Raman linewidths are strongly dependent on the gas temperature, the pressure, and the collision partners (see, e.g., [25]). Constant or unsuitable values may lead to inaccurate measurement results [26]. Up until now, only very few CARS experiments for multi-species detection, including water vapor, have been performed. Eckbreth et al. used either a dual broadband Stokes for a simultaneous detection of N<sub>2</sub>, CO<sub>2</sub>, and H<sub>2</sub>O, a dual-pump Stokes approach for a simultaneous measurement of N<sub>2</sub>, H<sub>2</sub>, and H<sub>2</sub>O, or a setup using several dye cells sequentially to measure N<sub>2</sub>, O<sub>2</sub>, CO, and H<sub>2</sub>O [27–29]. Simultaneous temperature and multi-species measurements were only possible with the first two approaches [27,28]. The dual broadband Stokes technique requires three laser beams of different frequencies, resulting in two two-color CARS processes and one three-color CARS process [27]. This results in independent signal intensity fluctuations of the H<sub>2</sub>O and N<sub>2</sub> CARS signals, which makes a concentration determination based on the absolute CARS signal intensities difficult. The dual-pump Stokes approach was used by Eckbreth et al. to detect N<sub>2</sub> and water vapor simultaneously. Nevertheless, since both CARS signals were partially spectrally overlapping on the detector, in this case, an evaluation was not performed [28]. Nishihara et al. used a VCARS approach to measure the temperature and the relative H<sub>2</sub>/H<sub>2</sub>O concentration simultaneously [30]. Here, the experimental spectra were compared with calculated H<sub>2</sub> and H<sub>2</sub>O spectra. Since precise Raman linewidth data are not available, they mentioned a relative error of 30% for the concentration determination.

All the above-mentioned approaches have used nanosecond laser systems. Simultaneous temperature and multi-species concentration measurements, including water vapor, have been demonstrated recently by Castellanos et al. [31] by using a hybrid femtoseconds/picoseconds rotational CARS system. This system was applied to an H<sub>2</sub>/air flame. In the first step, the temperature, the relative N<sub>2</sub>/O<sub>2</sub>, and the relative N<sub>2</sub>/H<sub>2</sub> concentrations were evaluated from the collision-free rotational CARS spectrum at a small probe delay. Taking this information into account, the water vapor concentration was then determined by studying the collider-dependent rotational energy transfer (RET) in the time domain between the coherently excited N<sub>2</sub> and all other molecules, including water vapor. However, no information concerning precision and accuracy for this method under well-defined

thermodynamic conditions has been given. In order to apply this approach, temperature and all species concentrations except water vapor have to be obtained independently from the RET, e.g., from the spectral signature. This is not easy in reactive flows, including hydrocarbons like methanation, since their rotational CARS signal is quite low. Furthermore, due to its spherical top symmetry, CH<sub>4</sub> even generates no rotational CARS signal (RCARS).

RCARS has previously been applied for water concentration measurement [32]. Unfortunately, the water's rotational CARS signal intensity was found to be five orders of magnitude weaker than the signal intensity of nitrogen, and RCARS is therefore unsuitable for water vapor concentration measurements in reacting flows [32].

This shows that, up to now, there is no suitable CARS technique for precise temperature and water vapor concentration measurements. Nevertheless, such a non-intrusive diagnostic tool is essential for the investigation of reactive flows, either in combustion or methanation processes. Therefore, we present a new concept for the development of a DPVCARS setup for the precise measurement of gas phase temperature and the relative water vapor-nitrogen concentration. Beside this, information concerning the precision and accuracy of this technique is presented.

## 2. DPVCARS Process

In DPVCARS, two narrowband pump lasers ( $\omega_{P1}$ ,  $\omega_{P2}$ ) in conjunction with a broadband Stokes laser ( $\omega_S$ ) are used to generate the CARS radiation of two spectral regions simultaneously. The frequency of the Stokes laser beam is tuned so that when it interacts with any of the two-pump laser beams, the differences between the respective frequencies equal the Raman resonances ( $\omega_{R1}$ ,  $\omega_{R2}$ ) of the molecules that are to be probed. From the two excited Raman polarizations at  $\omega_{P1} - \omega_S$  and  $\omega_{P2} - \omega_S$ , the pump beams  $\omega_{P2}$  and  $\omega_{P1}$  are scattered and form the CARS signals ( $\omega_{AS1}$ ,  $\omega_{AS2}$ ) at essentially the same frequency, following energy conservation given in Equation (1):

$$\omega_{AS1} = \omega_{P1} - \omega_S + \omega_{P2} \text{ and } \omega_{AS2} = \omega_{P2} - \omega_S + \omega_{P1} \quad (1)$$

However, as the Stokes laser is a broadband source,  $\omega_{AS2}$  can be tuned within the bandwidth of  $\omega_S$  to separate the two signals spectrally. Detailed information can be found, e.g., in [14]. This technique has two main advantages. The generated CARS signals have almost the same frequency ( $\omega_{AS1} \approx \omega_{AS2}$ ) since a common broadband Stokes laser is used and thus can be detected by one spectrometer and one CCD camera. DPVCARS signals are not affected by the relative power fluctuations of the different laser beams since both signals are generated by the same three beams, as shown in Equation (2). The energy level diagram for the DPVCARS system interacting with two different molecules with Raman resonances  $\omega_{R1}$  and  $\omega_{R2}$  is shown in Figure 1.

$$I_{AS1} \sim I_{P1} I_S I_{P2} \text{ and } I_{AS2} \sim I_{P2} I_S I_{P1} \quad (2)$$

For simultaneous temperature and relative water vapor-nitrogen concentration measurements using the DPVCARS technique, Q-branch vibrational Raman resonances of water ( $3657 \text{ cm}^{-1}$ ) and nitrogen ( $2331 \text{ cm}^{-1}$ ) were considered [5]. Water vapor is a triatomic molecule with three vibrational Raman active modes: the symmetric stretch, which is the dominant mode  $\nu_1$  ( $3657.1 \text{ cm}^{-1}$ ), the antisymmetric stretch  $\nu_2$  ( $3755.9 \text{ cm}^{-1}$ ), and the bending mode  $\nu_3$  ( $1594.7 \text{ cm}^{-1}$ ) [5]. Since it is a complex molecule with interactions between various vibrational and rotational states, collisional linewidth is not well known, and spectral fitting methods may lead to inaccurate concentration values. Therefore, a calibration method using known binary mixtures of water vapor and nitrogen is most preferable. Such a calibration method has been used previously for the determination of fuel/air ratios in an ethene-air flame [20].

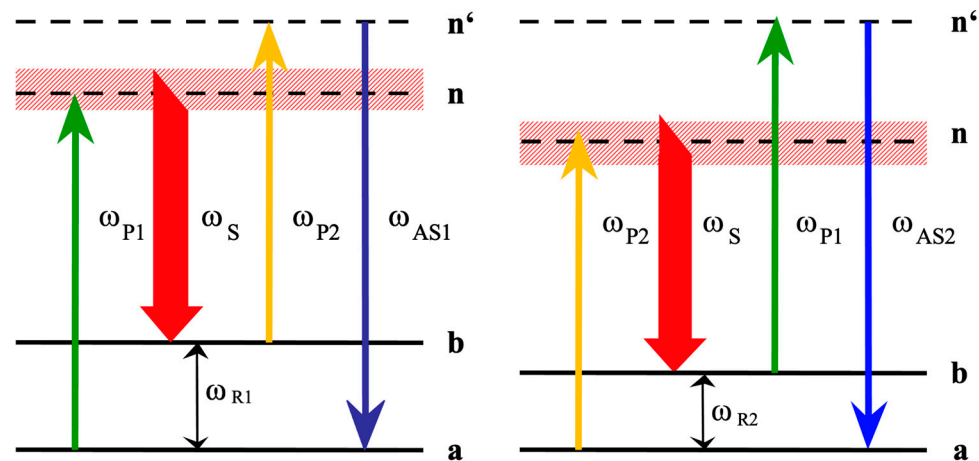


**Figure 1.** Energy level diagram for a dual-pump VCARS process: a is the ground energy state, b is the excited state, and n and n' are the virtual energy states.

### 3. Experimental

#### 3.1. DPVCARS System

A scheme of the experimental DPVCARS setup is illustrated in Figure 2. For the CARS setup, a seeded frequency-doubled neodymium-doped yttrium aluminum garnet laser (Nd:YAG, Spectra Physics GCR 270-10, 532 nm, 8 ns, 10 Hz, max. pulse energy: 800 mJ, spectral bandwidth (FWHM):  $0.003 \text{ cm}^{-1}$ ) was used. The Nd:YAG laser was used as a pump source for a broadband ( $\omega_S$ ) and a narrowband dye laser ( $\omega_{P2}$ ). A third part of the Nd:YAG laser beam provided the pump beam ( $\omega_{P1}$ ) for the CARS process. About 12% of the Nd:YAG output energy was used as the pump beam for the CARS process. 33% of the energy was deployed to pump the narrowband dye laser (Radiant Dyes NarrowScanK) and 55% to pump the broadband dye laser (Radiant Dyes RDP-1S). The narrowband dye laser was operated with a mixture of Rhodamine 6G (0.14 g/L) and Pyrromethene 597 (0.16 g/L) dissolved in ethanol, generating a tunable laser beam with a wavelength range of 572 to 578 nm and a bandwidth of  $0.03 \text{ cm}^{-1}$ . A mixture of Pyridine-1 (0.3 g/L) and DCM (0.3 g/L) dissolved in ethanol was used to generate a broadband dye laser profile with a central wavelength of 660 nm and a full width at half maximum (FWHM) of  $270 \text{ cm}^{-1}$ .

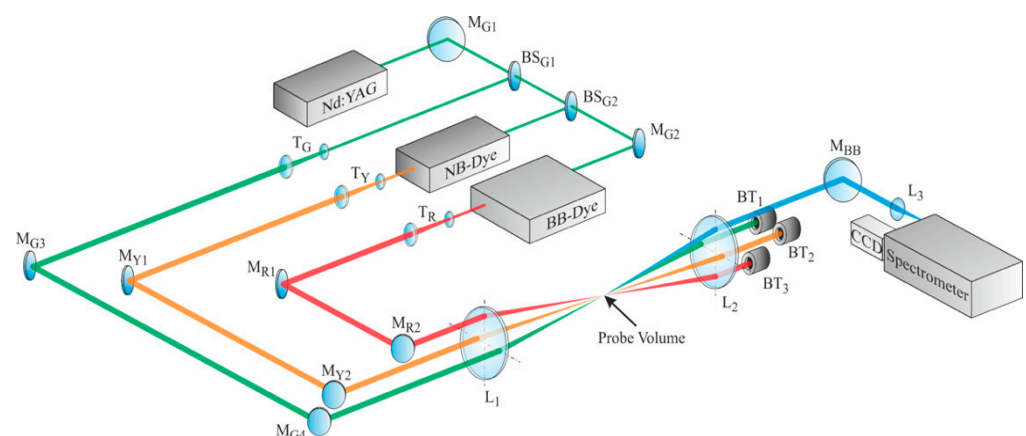


**Figure 2.** Schematic representation of the experimental DPVCARS setup: BB-Dye: Broadband dye laser; BS: Beam splitter; BT: Beam trap; CCD: charge-coupled device camera; L: Lens; M: Mirror; NB-Dye: Narrowband dye laser; Nd:YAG; T: Galileo telescope.

The maximum pulse energies for the DPVCARS process were 30 mJ for each of the three beams. Two  $f = 500$  mm lenses were used for focusing and recollimating the beams in a folded BOXCARS configuration, as shown in Figure 3. The folded BOXCARS geometry was used to ensure a suitable spatial resolution and enhanced spatial separation of the CARS signal. The probe volume was measured to be 2 mm in length and  $150 \mu\text{m}$  in diameter. The center of the gas cell was placed at the focal point of the two lenses labeled as the probe volume in the schematic representation in Figure 2. At the probe volume, a fourth beam, the CARS signal, was generated with a frequency of  $\omega_{AS}$ , corresponding to a wavelength of approximately 473 nm. The CARS signal was focused by a lens ( $f = 125$  mm) to the entrance slit (0.15 mm) of a spectrometer (Horiba iHR550,  $f=550$  mm) equipped with a 2400 lines/mm grating. A 14-bit charge-coupled device (PCO pco.2000, CCD,  $2048 \times 2048$ -pixel) with a pixel size of  $7.4 \times 7.4 \mu\text{m}^2$ ) was used to record the spectra. The combination of the spectrometer and the CCD camera is resulting in a spectral resolution of  $0.284 \text{ cm}^{-1}/\text{pixel}$  (with a horizontal binning of 2 pixels) and a spectral coverage of about  $400 \text{ cm}^{-1}$ .

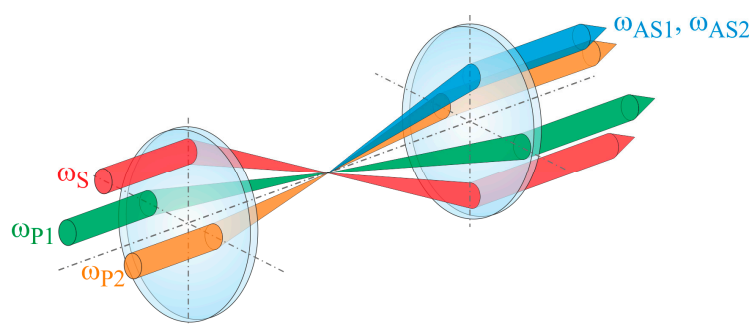


**Figure 3.** A schematic representation of folded BOXCARS geometry.

### 3.2. Heatable Gas Cell

For the investigation of the different water vapor–nitrogen mixtures, a cylindrical stainless-steel cell with a length of 400 mm, an internal diameter of 35 mm, and an outer diameter of 55 mm was used. The cell was equipped with optical NBK7 glass windows at both ends for optical access. It was provided with inlet lines for the gases and a connection to a pressure sensor to measure the absolute pressures. The gas cell was operated at temperatures up to 723 K and at atmospheric pressure, covering the range of conditions typical for a synthetic methanation process.

A heating tape in combination with a temperature controller was used to heat the insulated gas cell to maintain it at a desired temperature. The inlet lines were also heated to avoid water vapor condensation. The temperature in the gas cell was monitored by a Ni-Cr-Ni (Type K) thermocouple installed in an immersion tube. Additionally, temperature profiles were recorded along the length of the cell to determine the region of constant temperature by using a thermocouple (Type K) with an accuracy of  $\pm 3$  K. The different temperature profiles are shown in Figure 4. It can be seen that the temperature remained constant for 40 mm around the center of the cell. Therefore, a constant temperature along the probe volume length of 2 mm, positioned in the center of the cell, can be assumed.

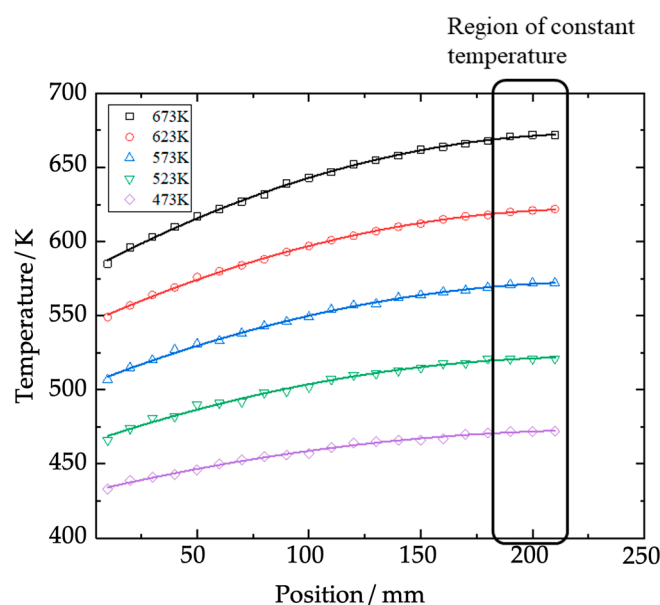


**Figure 4.** Thermocouple temperature profiles measured from one end to the center of the cell.

### 3.3. Temperature Evaluation and Mixture Preparation

With the DPVCARS setup, 500 single-pulse CARS spectra were acquired at different temperatures for different water vapor–nitrogen mixtures. In the first step, the recorded experimental spectra were background-corrected, averaged, and normalized against the non-resonant CARS spectra of argon to compensate for the spectral profile of the broadband dye laser. The temperature in the probe volume was determined from the  $N_2$  vibrational CARS part of the spectrum by using a least-squares fitting procedure against a library of theoretically calculated spectra. An in-house-developed CARS code was used to generate a pre-calculated library of  $N_2$  spectra for different thermodynamic conditions. The Raman linewidths were included via the modified exponential gap (MEG) law with the parameters given by Rahn and Palmer [33].

In the next step, relative water vapor–nitrogen concentrations were determined using a calibration procedure. The calibration curves were generated by comparing the square root of the integrated intensity ratios of the different binary mixtures prepared in the gas cell at different temperatures. The square root of the integrated intensity ratios is used because the CARS signal intensities are proportional to the square modulus of the third-order susceptibility, which is directly proportional to the number density of the species [5].

For the calibration procedure, four binary mixtures of water vapor and nitrogen were prepared inside the heatable gas cell. For each mixture, liquid water was introduced by a syringe through a rubber septum into the heated and evacuated gas cell. Due to the elevated temperature in the evacuated cell ( $T \geq 473$  K) the introduced water completely evaporated. The resulting partial water vapor pressure was recorded. Thereafter, a binary mixture was created in the cell by introducing nitrogen up to a total pressure of 1000 hPa. The prepared binary mixtures contained water vapor at 24%, 32%, 37%, and 46%, respectively. The partial pressure was measured by a pressure sensor with an accuracy of 2% of the full range of up to 2.5 bar. CARS spectra were recorded for each of the prepared binary mixtures over a temperature range from 473 K to 673 K with increments of 50 K at 1000 hPa.

## 4. Results and Discussion

### 4.1. Experimental $N_2$ – $H_2O$ Spectra

Different DPVCARS spectra averaged over 500 single shots, background-corrected, and normalized are shown in Figure 5. The dye laser frequencies were adjusted to position the water vapor CARS signal at a wavenumber of  $21,200\text{ cm}^{-1}$ , while the  $N_2$  signal is positioned to a wavenumber of  $21,150\text{ cm}^{-1}$ . This allowed us to detect the two spectral

regions with one single spectrometer and one CCD camera [18]. Figure 5a,b demonstrates the effect of different species concentrations on the relative CARS signal intensities. An increase in water vapor concentration from 24% to 32% at a constant temperature results in approximately a squared proportional increase in the integrated signal intensity due to the dependence on the square modulus of the third-order susceptibility ( $\chi^{(3)}$ ), which is directly proportional to the number density of the species in the probe volume.

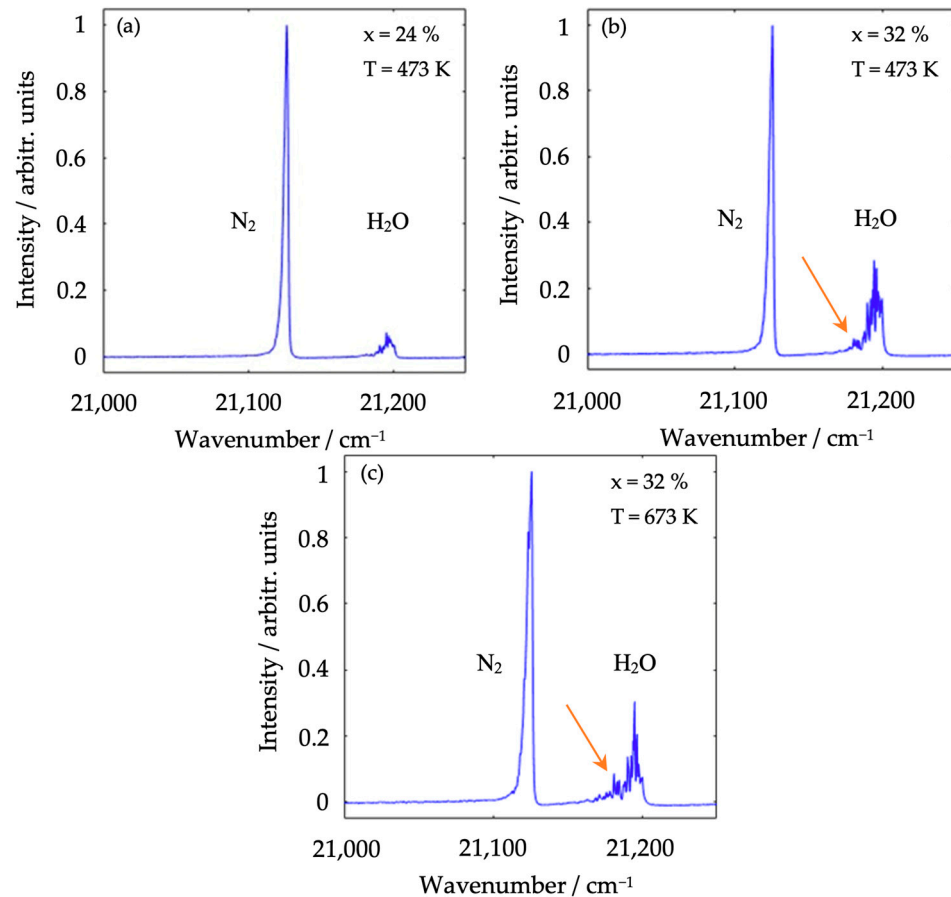


**Figure 5.** DPVCARS spectra for different water vapor and nitrogen mixtures at different temperatures (total pressure: 1000 hPa): (a) 24% water vapor at 473 K; (b) 32% water vapor at 473 K; and (c) 32% water vapor at 673 K.

By comparing Figure 5b,c the CARS signal dependence on temperature can be seen. The spectrum of H<sub>2</sub>O at elevated temperatures exhibits a pronounced contribution to the low-wavenumber part of the spectrum (highlighted by the red arrows). This is attributed to the CARS signal intensity increase of the higher rotational lines due to the temperature rise. Furthermore, thermal excitation of higher rotational states [5] leads to an apparent broadening of both the H<sub>2</sub>O and N<sub>2</sub> spectra. Based on these trends, it is possible to determine temperature and concentration in nitrogen–water vapor mixtures simultaneously. For this purpose, a calibration procedure is developed in the following section.

#### 4.2. Calibration Procedure

After processing the spectra as outlined in the section “Temperature evaluation and mixture preparation”, the calibration procedure outlined by Lucht et al. [19] and Beyrau et al. [20] for fuel/nitrogen calibration curves in combustion applications was used. To this end, the square root of the ratio of VCARS intensities  $I_{AS}$  of water vapor and nitrogen, each integrated over the frequency  $\omega$ , was plotted against the H<sub>2</sub>O concentration according to Equation (3).

$$\left( \frac{\int_{\omega, \text{Water vapor}} I_{AS1} d\omega}{\int_{\omega, \text{Nitrogen}} I_{AS2} d\omega} \right)^{1/2} \quad (3)$$

The fuel concentration is quite small, as is its variation. In this case, the calibration curves can be assumed to be nearly linear. The situation is different for water vapor. Here, calibration curves over a large water vapor concentration range are required [4].

Figure 6 shows the determined calibration curves for the four gas mixtures at temperatures of 473 K, 523 K, 573 K, 623 K, and 673 K. The calibration measurements indicate that with increasing water vapor concentration in the measured parameter range, the CARS intensity of the water signal exhibited an exponential increase. Note that the calibration curve in [20] appears to be linear due to the small concentration range. It can also be seen that the integrated intensity ratio is reducing with increasing temperature for a particular water vapor concentration. A reason is that with increasing temperature, there are much more rovibrational energy levels of water vapor involved in the VCARS process than for nitrogen. It is important to note that, theoretically, all curves should start from zero, since the CARS signal is proportional to the concentration of the molecule. The calibration curves can be generally described by polynomial Equation (4), where  $x$  represents the water vapor concentration and  $y$  represents the integrated intensity ratio. The coefficient of determination ( $R^2$ ) of all polynomial fits was  $>0.99$ , indicating a high correlation between the model predictions and the measured data.

$$y = B1x + B2x^2 \quad (4)$$

In Figure 7, the development of the coefficients  $B1$  and  $B2$  with temperature is shown. It is obvious that the coefficient  $B2$  remains nearly constant ( $B2 = 6.45 \times 10^{-4}$ ) and the coefficient  $B1$  displays a linearly decreasing trend with temperature. Thereby, the square root of the CARS intensity ratio can be described for an arbitrary temperature and water vapor concentration within the calibrated data range.

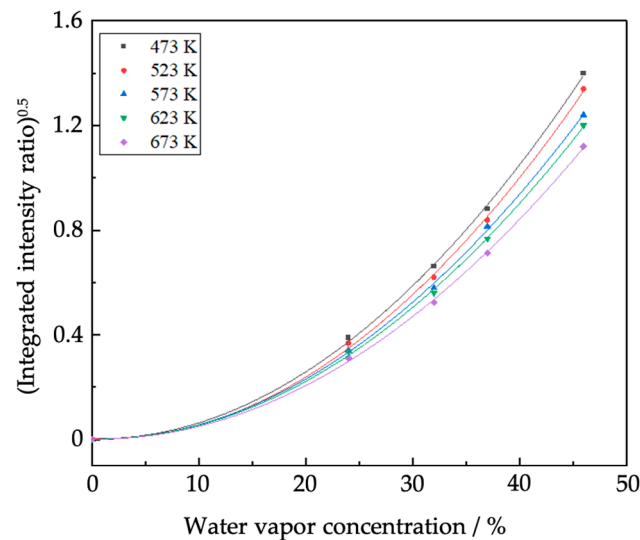


**Figure 6.** Water vapor–nitrogen calibration curves for different temperatures.

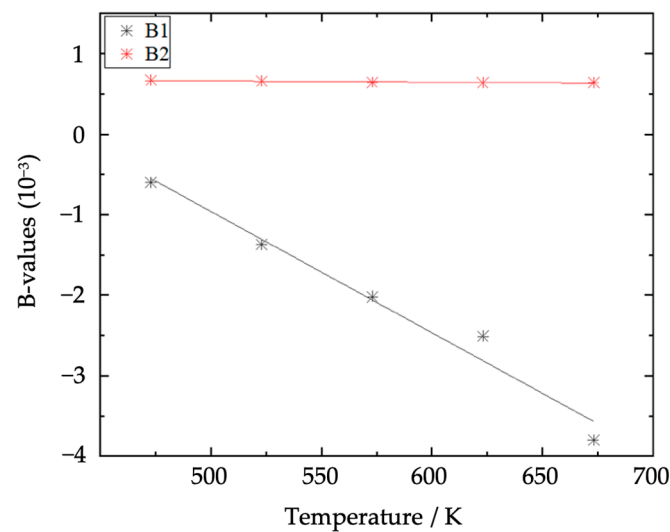


**Figure 7.** Development of the B1 and B2 values with temperature.

#### 4.3. Validation Measurements

To validate the DPVCARS system, a known binary mixture was analyzed at a fixed temperature of 553 K. At this temperature inside the cell, a binary mixture containing water at a partial pressure of 260 hPa and a total pressure of 1000 hPa (26% water vapor) was investigated by the acquisition of 500 single pulse spectra. In the first step, the gas temperature was determined by using the N<sub>2</sub> band of each spectrum. The least squares contour fitting procedure described in the section “Temperature evaluation and mixture preparation” was applied. Figure 8 shows an evaluated N<sub>2</sub> VCARS single pulse spectrum (blue) together with the corresponding best-fitting theoretical spectrum (red). The evaluated temperature of the spectrum was 551 K. For 500 single pulse spectra, a mean temperature of 550 K and a standard deviation of 4.9% were determined. The temperature performance of this setup concerning accuracy and precision is comparable to that of other VCARS systems described in the literature (see, e.g., [13]).

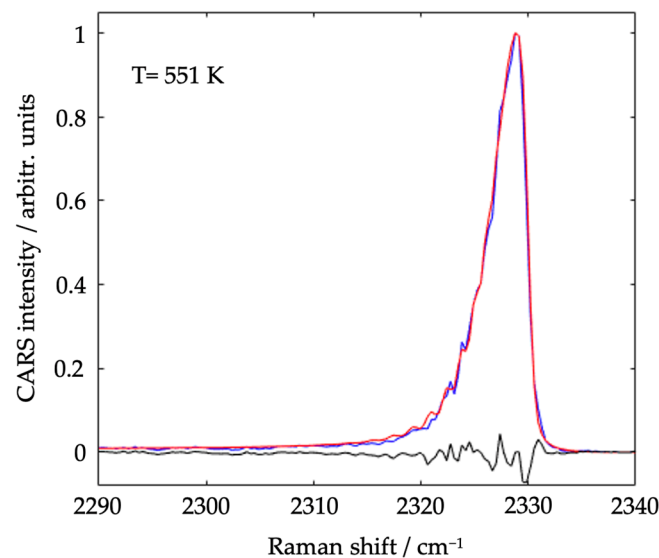


**Figure 8.** Single-pulse N<sub>2</sub> VCARS spectrum (blue) shown together with the corresponding best-fitting theoretical spectrum (red). The difference is the black curve.

In the next step, the coefficients B1 and B2 for this temperature are determined from Figure 7 as:

$$B1 = -1.769 \times 10^{-3}$$

$$B2 = 6.464 \times 10^{-4}$$

From Equation (4), a new calibration curve for the N<sub>2</sub> CARS temperature of 550 K is calculated, as shown in Figure 9. The square root of the integrated intensity ratio for this experiment was determined to be 0.39, resulting in a relative water vapor concentration of 25.8% for the binary mixture. This measurement result agrees very well with the set binary mixture of 26% water vapor.

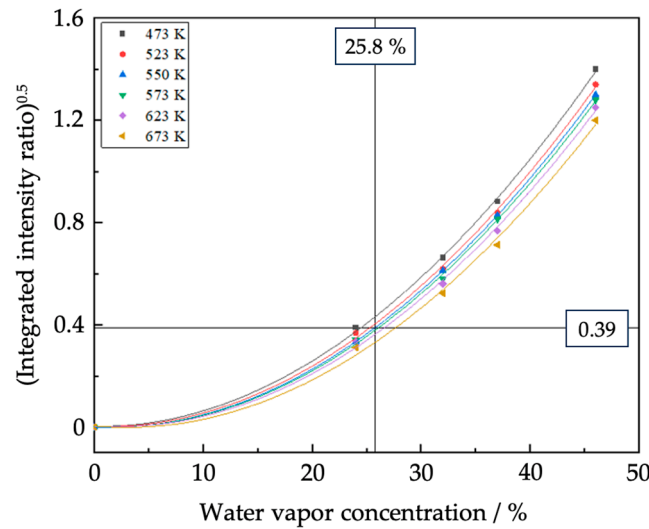


Figure 9. Determination of relative water-nitrogen concentration at 550 K.

To determine the accuracy and precision of the developed CARS system, 500 single pulse spectra of this binary gas mixture were processed individually by the procedure described above. With the resulting matrix of integrated intensity ratios for each single shot, relative water concentrations were determined. These relative concentrations were then used to achieve a probability distribution (PDF) of the measured concentration, as shown in Figure 10. The determined mean value of the water vapor concentration was 25.8% with a relative standard deviation of 5.7%, which is comparable with the results of the relative oxygen and ethene concentrations given in [20].

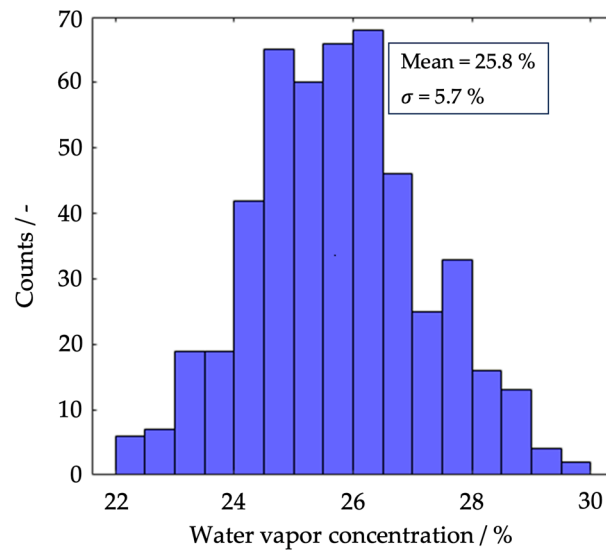


Figure 10. Probability distribution function of 500 single pulse spectra acquired for a water vapor-nitrogen mixture of 26% water vapor and a thermocouple temperature of 553 K.

## 5. Conclusions

A DPVCARS system has been set up and tested successfully for simultaneous temperature and relative water vapor–nitrogen concentration measurements. The dye laser frequencies were adjusted to position the spectrum of the CARS signals of the two molecules close to each other, enabling detection by one detection system. This allowed the measurement of the relative water vapor–nitrogen concentration by comparing the CARS signal intensities. The temperature was determined from the nitrogen signature in the spectrum by applying a contour fit procedure. The single-pulse performance of this CARS system was successfully validated by determining the concentration of a known binary mixture containing 26% water vapor at a thermocouple temperature of 553 K. In this case, a mean CARS temperature of 550 K and a mean water vapor concentration of 25.8% were achieved. The results confirm the effectiveness of the DPVCARS system in accurately determining temperatures and gas concentrations in a known binary mixture. The high agreement with expected values and low relative standard deviation in temperature (4.9%) and concentration (5.7%) in the measurements underscore the reliability of this approach. The precision and accuracy attained by this new concept make it suitable for deployment in reactive flows.

**Author Contributions:** Conceptualization, T.S.; methodology, E.S., A.T., Y.H. and T.S.; software, E.S., A.T. and Y.H.; validation, E.S.; formal analysis, E.S. and T.S.; investigation, E.S., A.T. and Y.H.; resources, T.S.; data curation, E.S. and A.T.; writing—original draft preparation, A.T.; writing—review and editing, E.S. and T.S.; visualization, E.S. and A.T.; supervision, T.S. and N.W.K.; project administration, T.S.; funding acquisition, T.S. All authors have read and agreed to the published version of the manuscript.

**Funding:** This research was funded by the German Science Foundation (DFG), grant number SE 804/8-1.

**Data Availability Statement:** The data presented in this study are available on request from the corresponding author. The data are not publicly available as they are part of an on-going study.

**Acknowledgments:** The authors of this work would like to sincerely acknowledge the financial support partially provided by the German Science Foundation (DFG) in the framework of the SPP2080 and the German Academic Exchange Service (DAAD). Also, support from the Center for Sensor Systems (ZESS) at the University of Siegen and the Dedan Kimathi University of Technology is gratefully acknowledged.

**Conflicts of Interest:** The authors declare no conflict of interest.

## References

1. Gao, J.; Liu, Q.; Gu, F.; Liu, B.; Zhong, Z.; Su, F. Recent advances in methanation catalysts for the production of synthetic natural gas. *RSC Adv.* **2015**, *5*, 22759–22776. [[CrossRef](#)]
2. Cassia, R.; Nocioni, M.; Correa-Aragunde, N.; Lamattina, L. Climate change and the impact of greenhouse gases: CO<sub>2</sub> and NO, friends and foes of plant oxidative stress. *Front. Plant Sci.* **2018**, *9*, 273. [[CrossRef](#)] [[PubMed](#)]
3. de Vasconcelos, B.R.; Lavoie, J.M. Recent advances in power-to-X technology for the production of fuels and chemicals. *Front. Chem.* **2019**, *7*, 392. [[CrossRef](#)] [[PubMed](#)]
4. Wulf, C.; Zapp, P.; Schreiber, A. Review of power-to-X demonstration projects in Europe. *Front. Energy Res.* **2020**, *8*, 191. [[CrossRef](#)]
5. Eckbreth, A.C. *Laser Diagnostics for Combustion Temperature and Species*, 2nd ed.; Gordon and Breach: Amsterdam, The Netherlands, 1996. [[CrossRef](#)]
6. Meng, H.; Ren, Y.; Cameron, F.; Pitsch, H. In-situ temperature and major species measurements of sooting flames based on short-gated spontaneous Raman scattering. *Appl. Phys. B* **2023**, *129*, 32. [[CrossRef](#)]
7. Kim, H.; Aldén, M.; Brackmann, C. Suppression of unpolarized background interferences for Raman spectroscopy under continuous operation. *Opt. Express* **2021**, *29*, 1048–1063. [[CrossRef](#)] [[PubMed](#)]
8. Steinberg, A.; Roy, S. (Eds.) *Optical Diagnostics for Reacting Flows: Theory and Practice*, 1st ed.; AIAA: Stuttgart, Germany, 2023. [[CrossRef](#)]
9. Klick, T.; Marko, K.A.; Rimai, L. Broadband single-pulse CARS spectra in a fired internal combustion engine. *Appl. Opt.* **1981**, *20*, 1178–1181. [[CrossRef](#)]
10. Alden, M.; Wallin, S. CARS experiments in a full-scale (10 × 10 m) industrial coal furnace. *Appl. Opt.* **1985**, *24*, 3434–3437. [[CrossRef](#)]

11. Clauss, W.; Klimenko, D.N.; Oschwald, M.; Vereschagin, K.A.; Smirnov, V.V.; Stelmakh, O.M.; Fabelinsky, V.I. CARS investigation of hydrogen Q-branch linewidths at high temperatures in a high-pressure H<sub>2</sub>–O<sub>2</sub> pulsed burner. *J. Raman Spectrosc.* **2002**, *33*, 906–911. [[CrossRef](#)]
12. Athmanathan, V.; Rahman, K.A.; Lauriola, D.K.; Braun, J.; Paniagua, G.; Slipchenko, M.N.; Sukesh, R.; Meyer, T.R. Femtosecond/picosecond rotational coherent anti-Stokes Raman scattering thermometry in the exhaust of a rotating detonation combustor. *Combust. Flame* **2021**, *231*, 111504. [[CrossRef](#)]
13. Seeger, T.; Leipertz, A. Experimental comparison of single-shot broadband vibrational and dual-broadband pure rotational coherent anti-Stokes Raman scattering in hot air. *Appl. Opt.* **1996**, *35*, 2665–2671. [[CrossRef](#)]
14. Lucht, R.P. Three-laser coherent anti-Stokes Raman scattering measurements of two species. *Opt. Lett.* **1987**, *12*, 78–80. [[CrossRef](#)] [[PubMed](#)]
15. Hancock, R.D.; Schauer, F.R.; Lucht, R.P.; Farrow, R.L. Dual-pump coherent anti-Stokes Raman scattering measurements of nitrogen and oxygen in a laminar jet diffusion flame. *Appl. Opt.* **1997**, *36*, 3217–3226. [[CrossRef](#)] [[PubMed](#)]
16. Frederickson, K.; Kearney, S.P.; Luketa, A.; Hewson, J.C.; Grasser, T.W. Dual-pump CARS measurements of temperature and oxygen in a turbulent methanol-fueled pool fire. *Combust. Sci. Technol.* **2010**, *182*, 941–959. [[CrossRef](#)]
17. Brüggemann, D.; Wies, B.; Zhang, X.X.; Heinze, T.; Knoche, K.-F. CARS Spectroscopy for Temperature and Concentration Measurements in a Spark Ignition Engine. In *Combustion Flow Diagnostics*; Durao, D.F.G., Whitelaw, J.H., Witze, P.O., Eds.; Kluwer Academic Pub.: Dordrecht, The Netherlands, 1992; pp. 495–511.
18. Roy, S.; Meyer, T.R.; Lucht, R.P.; Afzelius, M.; Bengtsson, P.E.; Gord, J.R. Dual-pump dual-broadband coherent anti-Stokes Raman scattering in reacting flows. *Opt. Lett.* **2004**, *29*, 1843–1845. [[CrossRef](#)] [[PubMed](#)]
19. Green, S.M.; Rubas, P.J.; Paul, M.A.; Peters, J.E.; Lucht, R.P. Annular phase-matched dual-pump coherent anti-Stokes Raman spectroscopy system for the simultaneous detection of nitrogen and methane. *Appl. Opt.* **1998**, *37*, 1690–1701. [[CrossRef](#)] [[PubMed](#)]
20. Beyrau, F.; Seeger, T.; Malarski, A.; Leipertz, A. Determination of temperatures and fuel/air ratios in an ethene-air flame by dual-pump CARS. *J. Raman Spectrosc.* **2003**, *34*, 946–951. [[CrossRef](#)]
21. Beyrau, F.; Datta, A.; Seeger, T.; Leipertz, A. Dual-pump CARS for the simultaneous detection of N<sub>2</sub>, O<sub>2</sub> and CO in CH<sub>4</sub>-flames. *J. Raman Spectrosc.* **2002**, *33*, 919–924. [[CrossRef](#)]
22. Weikl, M.C.; Seeger, T.; Hierold, R.; Leipertz, A. Dual-pump CARS measurements of N<sub>2</sub>, H<sub>2</sub>, and CO in a partially premixed flame. *J. Raman Spectrosc.* **2007**, *38*, 983–988. [[CrossRef](#)]
23. Tedder, S.A.; Wheeler, J.L.; Cutler, A.D.; Danehy, P.M. Width-Increased dual-pump enhanced coherent anti-Stokes Raman spectroscopy. *Appl. Opt.* **2010**, *49*, 1305–1313. [[CrossRef](#)]
24. Hall, R.J.; Shirley, J.A.; Eckbreth, A.C. Coherent anti-Stokes Raman spectroscopy: Spectra of water vapor in flames. *Opt. Lett.* **1979**, *4*, 87–89. [[CrossRef](#)]
25. Misoi, H.; Hölzer, J.I.; Seeger, T. Temperature dependent determination of the S-branch Raman linewidths of oxygen and carbon dioxide in an oxyfuel relevant mixture. *Appl. Opt.* **2021**, *60*, 4410–4417. [[CrossRef](#)] [[PubMed](#)]
26. Hölzer, J.I.; Meißner, C.; Seeger, T. Improvement of the coherent model function for S branch Raman linewidth determination in oxygen. *Appl. Opt.* **2021**, *60*, C76–C83. [[CrossRef](#)] [[PubMed](#)]
27. Eckbreth, A.C.; Anderson, T.J. Dual broadband CARS for simultaneous, multiple species measurements. *Appl. Opt.* **1985**, *24*, 2731–2736. [[CrossRef](#)] [[PubMed](#)]
28. Eckbreth, A.C.; Anderson, T.J.; Dobbs, G.M. Multi-color CARS for hydrogen-fueled scramjet applications. *Appl. Phys. B Photophys. Laser Chem.* **1988**, *45*, 215–223. [[CrossRef](#)]
29. Eckbreth, A.C.; Dobbs, G.M.; Stufflebeam, J.H.; Tellex, P.A. CARS temperature and species measurements in augmented jet engine exhausts. *Appl. Opt.* **1983**, *23*, 1328–1339. [[CrossRef](#)] [[PubMed](#)]
30. Nishihara, M.; Freund, J.B.; Glumac, N.G.; Elliott, G.S. Dual-pump CARS measurements in a hydrogen diffusion flame in cross-flow with AC dielectric barrier discharge. *PSST* **2018**, *27*, 035012. [[CrossRef](#)]
31. Castellanos, L.; Mazza, F.; Bohlin, A. Water vapor in hydrogen flames by time-resolved collisional dephasing of the pure-rotational N<sub>2</sub> CARS signal. *Proc. Combust. Inst.* **2023**, *39*, 1279–1287. [[CrossRef](#)]
32. Nordström, E.; Bohlin, A.; Bengtsson, P.E. Pure rotational coherent anti-Stokes Raman spectroscopy of water vapor and its relevance for combustion diagnostics. *J. Raman Spectrosc.* **2013**, *44*, 1322–1325. [[CrossRef](#)]
33. Rahn, L.A.; Palmer, R.E. Studies of nitrogen self-broadening at high temperature with inverse Raman spectroscopy. *J. Opt. Soc. Am. B* **1986**, *3*, 1164–1169. [[CrossRef](#)]

**Disclaimer/Publisher’s Note:** The statements, opinions and data contained in all publications are solely those of the individual author(s) and contributor(s) and not of MDPI and/or the editor(s). MDPI and/or the editor(s) disclaim responsibility for any injury to people or property resulting from any ideas, methods, instructions or products referred to in the content.